PROPERTIES OF THE MOLECULAR TRANSPORT OF DISSOCIATED AND IONIZED GAS MIXTURES

I. A. Sokolova and G. A. Tirskii

UDC 533.539

Questions of the study of the molecular transport properties of low-density multicomponent partially dissociated and ionized gas mixtures, particularly air, have received much attention, associated with the solution of many practical problems that occur in investigations of high-temperature gasdynamic processes proceeding in multicomponent mixtures. Required for their solution is extensive information on both the thermodynamic and transport properties of the mixtures in broad temperature and pressure ranges. Since algorithms for the solution of gas dynamics problems are highly accurate at this time, the initial data on the physical properties (coefficients of the equations) should not concede to the total accuracy requirements of the solutions of the hydrodynamics equations themselves.

Extensive material, obtained as a result of experiments and numerical computations that permit the analysis of possible errors admitted in the numerical computations of the transport properties, has been accumulated on the initial molecular data for the computation of the thermophysical and transport properties of air and its main components. In contrast to the experimental data on transport properties that represent information at individual temperature points and, as a rule, at one pressure, the numerical computations of the transport coefficients themselves can be performed in broad temperature and pressure ranges to an accuracy no worse than ~1%. The accuracy of the numerical computations performed on the basis of the molecular-kinetic theory by the Chapman–Enskog method using series expansions in Sonine polynomials [1, 2] is determined by the number of terms retained [3-6].

The main error source in calculating the transport properties is the incompleteness of the information on interaction of the particles of the mixture components. No universal facilities exist for obtaining the particle interaction potentials in the whole domain of intramolecular spacings. Known methods of obtaining information from both processing of experimental data (for instance, by beam scattering, viscosity measurements, virial coefficients, the states of solid bodies, etc.) and using quantum mechanical computations afford a description of just part of the potential curve in a limited range of intramolecular spacings R. To obtain a complete potential it is necessary to merge the potential functions, which is done by using splines. Moreover, the problem remains of filling in the missing data for a number of components. Therefore, the collision integrals, the triple integrals in whose terms the transport coefficients are expressed in the long run, contain indeterminacies associated with the methods used to obtain the potentials. Examination of the most extensive methods used for computations of the collision integrals of atoms, ions, and molecules permits analysis of the influence of the existing spread in the collision integrals of individual pairs of components on the viscosity and heat conduction coefficients in different temperature bands for air and nitrogen, comparison with experiments, and establishment of limits of possible deviations of the numerical computations from the most fiduciary results. This analysis is indeed represented in this paper.

1. EXACT EXPRESSIONS OF THE VISCOSITY AND HEAT CONDUCTION COEFFICIENTS

The method for computing the transport coefficients of multicomponent rarefied gas mixtures and plasma is developed in [1, 2, 5-7]. Underlying the theory of transport phenomena is the Boltzmann kinetic equation and the resulting transport equation and kinetic coefficients. Under the assumption of a small deviation of the component distribution functions from the Maxwell distribution, the theory of transport phenomena of partially ionized mixtures [7] yields results that agree formally with the results of the classical Chapman–Enskog (C–E) theory: the transport coefficients determined by the C–E method when using the Boltzmann collision term are equivalent to the results of expansions in Sonine polynomials based on application of the Fokker–Planck collision term if a Coulomb shielded potential is

---

Moscow. Translated from Zhurnal Prikladnoi Mekhaniki i Tekhnicheskoi Fiziki, No. 3, pp. 14-28, May-June, 1988. Original article submitted January 27, 1987.

0021-8944/88/2903-0326$12.50

selected as the charged particle interaction. In the limit of a fully ionized gas, the solution found in the Sonine polynomial expansion and utilization of the Coulomb shielded potential is in agreement with the numerical solution of the Fokker–Planck equation [8]. Depending on the number of terms ξ retained in the Sonine polynomial expansion, the transport coefficients have the following expressions:

Viscosity coefficient in a second approximation

$$\mu(2) = -\frac{5}{2}\frac{1}{\det\|\widehat{\mathbf{q}}_{rs}\|}\begin{vmatrix} 0 & x_s\sqrt{m_s} & 0 \\ x_r\sqrt{m_r} & \widehat{\mathbf{q}}_{rs}^{0,0} & \widehat{\mathbf{q}}_{rs}^{0,1} \\ 0 & \widehat{\mathbf{q}}_{rs}^{1,0} & \widehat{\mathbf{q}}_{rs}^{1,1} \end{vmatrix}, \tag{1.1}$$

$$\widehat{q}_{ij}^{m,p} = \sqrt{\frac{m_j}{2\pi kT}}\left\{8x_i\left(\frac{m_i}{m_j}\right)^{p+1}\sum_{k=1}^{N} x_k\sum_{l=1}^{m+1}[\delta_{ij} + (-1)^l\,\delta_{jk}]\sum_{t=0}^{m}\frac{\left(\dfrac{m_j}{m_k}\right)^{2t+[1-(-1)^l]/2}}{\left(\dfrac{m_i}{m_k}+1\right)^{m+p+3/2}}\sum_{s=l}^{m+p+l-2t} b_{lts}^{m,p}\left[\pi\overline{Q}_{ik}^{(l,s)}(T)\right]\right\};$$

Transport heat conduction coefficient in a third approximation

$$\lambda(3) = -\frac{75}{8}\frac{k}{\det\|\mathbf{q}_{rs}\|}\begin{vmatrix} 0 & x_s & 0 \\ x_r & \mathbf{q}_{rs}^{1,1} & \mathbf{q}_{rs}^{1,2} \\ 0 & \mathbf{q}_{rs}^{2,1} & \mathbf{q}_{rs}^{2,2} \end{vmatrix}, \tag{1.2}$$

$$q_{ij}^{m,p} = \sqrt{\frac{m_j}{2\pi kT}}\left\{8x_i\left(\frac{m_i}{m_j}\right)^{p+1/2}\sum_{k=1}^{N} x_k\sum_{l=1}^{m+1}[\delta_{ij} + (-1)^l\,\delta_{jk}]\times\right.$$

$$\left.\times\sum_{t=0}^{m+1-l}\left(\frac{m_j}{m_k}\right)^{2t+l-1}\frac{1}{\left(\dfrac{m_i}{m_k}+1\right)^{m+p+1/2}}\sum_{s=l}^{m+p-(l-2)-2t} a_{lts}^{m,p}\left[\pi\overline{Q}_{ik}^{(l,s)}(T)\right]\right\}$$

$$(a_{101}^{1,1} = 25/4,\ a_{102}^{1,1} = -15,\ a_{103}^{1,1} = 12,\ a_{111}^{1,1} = 30/4,\ a_{202}^{1,1} = 4,\ a_{101}^{1,2} = 175/16,$$
$$a_{102}^{1,2} = -315/8,\ a_{103}^{1,2} = 57,\ a_{104}^{1,2} = -30,\ a_{111}^{1,2} = 420/16,\ a_{112}^{1,2} = -63/2,$$
$$a_{202}^{1,2} = 14,\ a_{203}^{1,2} = -16,\ a_{101}^{2,2} = 1225/64,\ a_{102}^{2,2} = -735/8,\ a_{103}^{2,2} = 399/2,$$
$$a_{104}^{2,2} = -210,\ a_{105}^{2,2} = 90,\ a_{111}^{2,2} = 5880/64,\ a_{112}^{2,2} = -1764/8,\ a_{113}^{2,2} = 162,$$
$$a_{121}^{2,2} = 1400/64,\ a_{202}^{2,2} = 49,\ a_{203}^{2,2} = -112,\ a_{204}^{2,2} = 80,\ a_{212}^{2,2} = 28,\ a_{303}^{2,2} = 24;$$
$$b_{101}^{0,0} = 10/3,\ b_{202}^{0,0} = 2,\ b_{101}^{0,1} = 35/3,\ b_{102}^{0,1} = -14,\ b_{202}^{1,0} = 7,\ b_{203}^{1,0} = -8,$$
$$b_{101}^{1,1} = 245/6,\ b_{102}^{1,1} = -98,\ b_{103}^{1,1} = 64,\ b_{111}^{1,1} = 140/6,\ b_{202}^{1,1} = 147/6,\ b_{204}^{1,1} = -40).$$

Here N is the total number of components in the mixture, x_i, m_i are the molar concentration and mass of the i-th particle, k is the Boltzmann constant, T is the mixture temperature, $Q_{ik}^{(\ell,s)}(T)$ are the collision integrals. The complete ("effective") heat conduction coefficient λ_{eff} for chemically and ionized equilibrium flows, whose magnitude is measured in experiments, is the sum $\lambda_{eff} = \lambda + \lambda_{int} + \lambda_R$, where λ_{int} is the heat conduction coefficient due to energy transferred by excited vibrational, rotational, and electron degrees of freedom of the particles [9], λ_R is the contribution to energy transport due to chemical dissociation and ionization reactions proceeding in equilibrium [10]:

$$\lambda_R = -\frac{1}{kT^2}\frac{1}{\det\|b_{ik}\|}\begin{vmatrix} 0 & Q_{L+1}^{\mathrm{T}} & \dots\ Q_N^{\mathrm{T}} \\ Q_{L+1}^{\mathrm{T}} & b_{L+1,L+1} & \dots\ b_{L+1,N} \\ \vdots & \dots & \\ Q_N^{\mathrm{T}} & b_{N,L+1} & \dots\ b_{N,N} \end{vmatrix};$$

L is the number of chemical elements in the mixture; N − L is the number of independent reactions, Q_i^{T} are quantities related to the heats of reaction, and b_{ij} are coefficients dependent on the diffusion properties of the components.

Convergence of the Sonine polynomial expansions in the calculation of the ionized gas transport coefficients was investigated by many authors [3, 7]. For air the convergence of all the transport coefficients and effective coefficients in the transport equation was studied in detail in [6, 10], where it is established by numerical computations of all the coefficients that it is necessary to evaluate $\lambda(\xi)$ for $\xi = 3$ and the viscosity coefficient $\mu(\xi)$

for $\xi = 2$ to assume 1% accuracy [a diminution of the number ξ by one results in an up to 60% error in the calculation of $\lambda(\xi)$ and up to 14% for $\mu(\xi)$ in the ionization domain]. For air not ionized the number of approximations for the computations of $\lambda(\xi)$ and $\mu(\xi)$ can be reduced: the first nonzero approximation $\lambda(2)$ and $\mu(1)$ assume accuracy of calculation not worse than 1%.

Experimental investigations of the transport properties of high-temperature gases (where molecule and atom dissociation and ionization processes start) were performed in [11-13] for air, and in [14-19] for nitrogen. A survey and analysis of the possible errors in the experimental results and the viscosity measurement methods are presented in [11] for high nitrogen and air temperatures. The maximal error of the experimental data is estimated at 50% for λ_{eff} measurements in the 6000-14,000 K temperature range by the authors of [12].

2. COLLISION INTEGRALS OF THE MAIN COMPONENTS OF AIR

The initial basis for the computation of the transport coefficients by the C−E method (1.1)-(1.2) is the mixture component composition x_i and the collision integrals $Q_{ij}^{(\ell,s)}(T)$ that are determined by computational means over the scattering cross section $Q_{ij}^{(\ell)}$ or by the pair interaction potentials $V_{ij}(R)$:

$$Q_{ij}^{(l,s)} = \frac{4(l+1)}{(s+1)!\,[2l+1-(-1)^l]}\int_0^\infty e^{-\gamma^2}\gamma^{2s+3}Q_{ij}^{(l)}(g)\,d\gamma,\quad \bar{Q}^{(l,s)} = \frac{Q^{(l,s)}}{\pi},$$

where $Q_{ij}^{(l)} = 2\pi\int_0^\infty [1-\cos^l\chi(b,g)]\,b\,db;\ \chi_{ij}(b,g) = \pi - 2b\int_{R_m}^\infty \frac{dR/R^2}{\left[1-\frac{b^2}{R^2}-\frac{2V(R)}{m_{ij}g^2}\right]^{1/2}}$; b is an alignment parameter, g is the relative velocity of the colliding particles at infinity, m_{ij} is the particle reduced mass, $\gamma^2 = m_{ij}g^2/2kT$, and R_m is the spacing of the smallest closure.

One of the directions in studying the interaction potentials of neutral mixture components is the restoration of the potential functions from measurement data for different physical properties in the liquid, solid, and gaseous phases including the traditionally utilized data on viscosity, heat conduction, virial coefficients, diffusion, etc. Used to determine the long-range portion of the potential are data of spectroscopic line measurement in microwave absorption and scattering spectra, measurement of rotational relaxation dispersion, and sound absorption sections, frequencies of anharmonic vibrations (mainly to obtain the potential in the area of the minimum of a potential well), measurement data on the states of solid bodies, crystalline lattice parameters, adhesion energy, phonon frequencies, etc. (for example, determination of the N_2-N_2 interaction potential [20]), data on thermal [21] and fast beam [22] scattering (one of the fundamental methods used to restore the interaction potential in the domain of repulsive forces), etc.

Another direction in the investigation of particle interaction potentials is a direct quantum mechanical computation. Quantum mechanical methods to study the long-range Van der Waals' forces, for whose computation first- and second-order perturbation theory methods are applied, have received the greatest development. By using a multipole expansion, the interaction energy is represented in the form of a series of reciprocal powers R^{-n}, where the first term of the series corresponds to different values of n depending on the state of the particles. Self-consistent field, configuration interaction, statistical methods based on using the Thomas−Fermi−Dirac and Thomas−Fermi functionals and the Gordon−Kim electron gas model developed later are applied for valence force computations. In principle, quantum mechanical methods were developed to take account of exchange and correlation forces, and the particle interaction can be computed in a broad range of intramolecular force actions for different electron configurations of different mutual orientation [23, 24].

In practice, to compute the transport properties it is expedient to have a spherically symmetric potential with a moderate number of variable parameters selected from the condition of greatest agreement with the results of processing of a number of diverse experimental properties. Simple model potentials of the Lennard-Jones model type, reciprocal power-law dependences, etc., are not always suitable for these purposes since some properties turn out to be responsive to the appearance of different intramolecular force domains: the Buckingham potential, restored by the viscosity coefficient, does not yield an adequate description of the results of thermal beam scattering [21] and conversely, the quadrupole terms in the interaction potential influence the second virial coefficient of nitrogen slightly [24], but terms up to R^{-10} and R^{-11} [25] are taken into account for the matching of the α and γ phases of the N_2 crystal with the crystal lattice properties (lattice parameters, adhesion energy, phonon frequencies, etc.) in nitrogen molecule interactions.

The interaction potentials of the molecules N_2-N_2, O_2-O_2, N_2-O_2 matched by a number of diverse properties (including test data on viscosity, on the second virial coefficients, self-diffusion, thermal diffusion, the zero choke-effect, etc.) are obtained in [26]. The long-range part of the potential is joined with the repulsion branch obtained from experiments on scattering [22] by using a cubic spline. For neutral N, O atoms in the ground states interacting with their ions N^+, O^+ the interaction potentials are computed by direct self-consistent field (SCF) quantum mechanical methods in [27], and in the electron gas model (EGM) in [28]. A survey of quantum mechanical methods of computing the interaction potentials of N, O atoms is presented in [26].

Besides the strict quantum mechanical computations, known for the determination of the interaction potentials between neutrals and their ions are a different kind of semiempirical theories and rules, computation using direct spectrum analysis data, the Rydberg–Klein–Rhys method, the atom–atom potentials (AAP) model, the model of overlapping ellipsoids, etc. In the AAP model which has received good confirmation by a number of direct quantum-mechanical computations and a comparison with experiments for certain systems the interaction potential of two molecular systems V(R) is expressed in terms of the atom–atom potential $V_{ij}(r_{ij})$ in the form $V(R)=\sum_{ij} V_{ij}(r_{ij})$, where r_{ij} is the spacing between atoms belonging to different molecules i and j. The average potential over the orientations $\langle V(R)\rangle$ is spherically symmetric; in particular we obtain for the exponential models $V_{ij}(r_{ij}) = A_{ij}\exp(-\alpha_{ij}r_{ij})$,

$$\langle V(R)\rangle = \sum_i \sum_j A_{ij} \frac{\exp(-\alpha_{ij}R)}{\alpha_{ij}^3 R a_i a_j} [(\alpha_{ij}R+2)\,\mathrm{sh}(\alpha_{ij}a_i)\,\mathrm{sh}(\alpha_{ij}a_j) \\ -(\alpha_{ij}a_i)\,\mathrm{ch}(\alpha_{ij}a_i)\,\mathrm{sh}(\alpha_{ij}a_j) - (\alpha_{ij}a_j)\,\mathrm{ch}(\alpha_{ij}a_j)\,\mathrm{sh}(\alpha_{ij}a_i)]$$

(a_i is the spacing between the atom and the center in the molecule i). Despite the broad application of the AAP model, the additivity principle underlying it is approximate since the molecule electron density is not a simple superposition of the electron densities of the atoms, its components. Consequently, the atom–atom potentials of the model do not agree with the interaction potentials of the isolated atoms, and additional investigations are required for their determination. For nonlinear and long linear molecules, the additive force model yields better agreement with experiments if the variable parameter d, the spacing to the force centers shifted in the molecule with respect to the equilibrium position of the atoms because of the inhomogeneous electron density distribution, is included in it. The spherically symmetric interaction potentials of atoms with the neutral N_2, O_2 molecules are obtained in [29].

The neutral-similar ion pairs represent a special kind of particle interaction. In contrast to the usual elastic scattering of atoms, molecules, and ions, the collision process between a neutral and the similar ion is accompanied by resonance charge-transfer which is treated from the classical viewpoint as charge transfer by an ion to an atom without energy exchange. This is manifest for the description of scattering in the fact that a particle deflected by an angle χ by the force center in the usual collision changes places with the partner in the collisions during charge exchange and is deflected an angle $\pi-\chi$. Such a process results in abrupt growth of the scattering section $Q^{(\ell)}$: for odd values of ℓ $Q^{(\ell)} = 2Q_{ex}$ (Q_{ex} is the resonance exchange section [30]). In the approximation of the perturbation theory of stationary states, the resonance exchange section can be expressed in terms of the resonance exchange probability P_{ex}, which is determined for slow collisions by the magnitude of the energy level splitting $\Delta E_{g,u} = E_g^+ - E_u^-$ of the quasimolecule term formed by the colliding particles

$$P_{\mathrm{ex}} = \sin^2\eta(b),\ \ \eta(b) = \frac{1}{hv}\int_{b_c}^{\infty} \frac{R\left[E_g^+(R) - E_u^-(R)\right]dR}{(R^2-b^2)^{1/2}},$$

where b is the alignment parameter, and v is the velocity of the colliding particles. Under the assumption of an exponential nature of the splitting energy dependence $\Delta E = A\exp(-\alpha R)$, an analytic expression $Q_{ex} = \pi b_c^2/2$ is obtained for the exchange section. Here b_c is found from the equation $(\pi A/hv)(\pi b_c/2\alpha)^{1/2}\exp(-\alpha b_c) = 1$. The exchange section obtained is approximated well by the semilogarithmic dependence $Q_{ex}^{1/2} \cong C_1 - C_2 \ln v$.

A survey of the exchange section of ions with the atoms of air components $N-N^+$, $O-O^+$ obtained by quantum mechanical methods of computing the splitting energy, semiempirical computation methods, and in experiments on the scattering of overtaking beams is presented in [26].

3. INFLUENCE OF EXISTING SPREAD IN COLLISION INTEGRALS OF MAIN AIR COMPONENTS ON THE VISCOSITY AND HEAT CONDUCTION COEFFICIENTS

Partially dissociated and ionized air is a complex multicomponent mixture containing atoms, molecules, molecular ions, and ions of atoms. The collision integrals of different pairs of air components N_2, O_2, N, O were computed in [4, 27, 31, 32] et al. At low temperatures (up to the beginning of air dissociation) the collisions of the neutral N_2 and O_2 components play the main role in the transport process. In this temperature range the collision integrals, computed by means of the potential obtained on the basis of consistent processing of a number of diverse experimental data and utilized for the computation of the transport properties, assure agreement with the experimental results on viscosity and heat conduction (air and nitrogen) to 1-2%. As the temperature grows and dissociation develops, the role of the molecular components drops in transport processes while the role of the mutual atom collisions and atom collisions with molecules grows. The collision integrals of the pairs N_2-N_2, $N-N_2$, N-N, and O-O are represented in Figs. 1-4. A comparison of the computation of $\bar{Q}^{(2,2)}$ by means of the potential [26] (curve 1) with the results of computations by the repulsive force potentials obtained from quantum mechanical computations [23] and in the AAP approximation [29] (curves 2 and 3) are presented in Fig. 1 for N_2-N_2. Represented in Fig. 2 are $N-N_2$ collision integrals computed by means of AAP potentials from [29] (curves 1 and 2, atomic potentials of isolated atoms from [28] are used to obtain the AAP potential in [2]) and found from scattering experiments [22] and by a semiempirical analysis [33] (curves 3 and 4). Represented in Figs. 3 and 4 are N-N and O-O collision integrals computed by means of the potentials obtained in the electron gas model approximation (EGM) [28], the Cubley potentials [32] (curves 1 and 2), from data in [33, 34] (curve 3) and averaged over the electron states of quasimolecules, converging to the lowest dissociation limit, from data in [27, 35] (curve 4). Deviations in the N_2-N_2 collision integrals because of different representations of the repulsion branch of the potentials from computations by the composite potential with a spline [26] are ~10%. The deviation in atom-atom collision integrals computed by the potentials in [33, 34], from computations by the EGM [28] are 15% for O-O atoms and 40% for N-N atoms. However, the spread in the atom-atom collision integrals computed by means of potentials from the strictest quantum mechanical representations by the SCF method and statistical EGM methods is not more than 1-3%. The discrepancy of computations in existing potentials for a number of air components can reach ~40% [29] in atom-molecule collision integrals but, exactly as for atom-atom components, real boundaries of the spread in collision integrals can be set up by an analysis of the most fiduciary data, which will be narrower than the boundaries of the total spread; these boundaries shift to ~15% in the atom-molecule case.

The $N-N^+$ collision integrals $\bar{Q}^{1,1}$ computed from Q_{ex} sections obtained by quantum mechanical computations by the SCF method [36-38], in the asymptotic theory approximation [39], the Heitler-London theory [40], and from experiments on beam scattering [41] are presented in Fig. 5 (curves 1-6, respectively). It is seen that the maximal spread in the collision integrals reaches two times, however the discrepancy in the collision integrals computed by means of [37-39] does not exceed ~10%.

Although there are computations at this time for the collision integrals of the air components performed by means of sufficiently reliable atom and molecule interaction potential functions [26], we analyze the influence of the existing spread in the data on collision integrals of different components on the change in the viscosity and heat conduction coefficients of chemically equilibrium nitrogen and air in different temperature ranges. Collisions of the neutral molecules N_2, O_2 play the main role in the transport process in chemically equilibrium mixtures at low temperatures (to the beginning of dissociation). Here the collision integrals computed by the potential found on the basis of consistent treatment of series of experimental data assure agreement with experiments on the viscosity and heat conduction of air and nitrogen to 1-2%. As the temperature rises and dissociation develops, the role of molecular collisions drops in the transport process while the role of mutual atom collisions and of atoms with molecules grows. The difference in molecule-molecule collision integrals because of the selection of the repulsion branch of the potential in

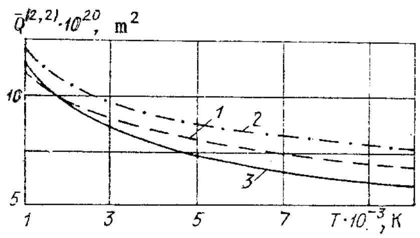

Fig. 1

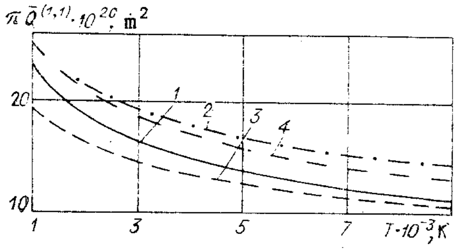

Fig. 2

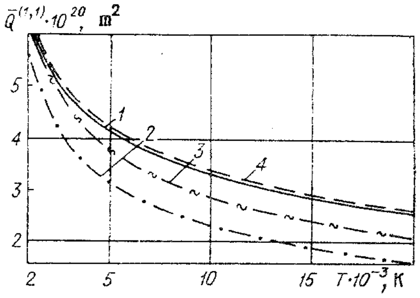

Fig. 3

computation of transport properties is not manifest at low temperatures and down to 2500 K. In the higher temperature range the difference in the molecule–molecule collision integrals due to the repulsion branch of the potential is leveled out by the presence of other components in the mixture. Presented in Table 1 are computations of the λ_{eff} and μ ($p = 1.013\cdot 10^5$ Pa) of air by the molecule–molecule collision integrals [26] (the repulsion branch of the potential is taken from experiments on scattering [22]) and collision integrals [29] (the repulsion branch of the potential is computed by the AAP model). The discrepancy in λ_{eff} is less than ~1% with the exception of the area of the first dissociation peak (T ~ 4000) where it is ~5%; the maximal discrepancy in the viscosity coefficient of air is still less (~3%).

Presented for comparison in Table 2 are computations of the viscosity coefficients of air ($p = 1.013\cdot 10^5$ Pa) by means of the Lennard-Jones [2] and Cubley [32] potentials (most often utilized in gasdynamic computations), by the potentials of [22, 29], and also the results of experimental measurements of the viscosity coefficient [42] having ~0.1% accuracy, and computations by means of integral collisions recommended in [26] (the deviation from experimental data in percents is indicated in the parentheses). In the temperature range to 2500 K the computations by means of the potentials [32] results in up to 10% error in the viscosity (and heat conduction λ_{eff}) coefficient, up to 5% by means of the Lennard-Jones potentials (the error in the transport coefficients calculated by means of the collision integrals for which the Lennard-Jones potential is used grows to tens of percents as the temperature rises), which indicates an imperfection in the approximation [32] and the Lennard-Jones model [2].

The influence of the spread in the atom–molecule collision integrals [that reaches ~20% for individual air components (see Fig. 2)] on the coefficients λ_{eff} and μ is represented in Table 3. The difference in the atom–molecule collision integrals, computed by the potentials [29] and restored from experiments on rapid beam scattering [22] (the potentials were restored by molecular pair scattering in which the atoms being investigated entered) results in a discrepancy in λ_{eff} to +7, +15% and in μ to +5, +10% in the 3000-7000 K temperature range. This is apparently associated with lowering of the collision integral values extrapolated into the low temperature range (below ~7000-5000 K) by using potentials found from experiments on fast beam scattering. On the other hand, the application of potentials obtained by the AAP model [29] and the AAP with potentials of isolated atoms results in a −10, −15% discrepancy in λ_{eff} and −3, −5% in μ. The use of AAP [29] nevertheless apparently assures accuracy no worse than ±5% in the λ_{eff} computations, as becomes evident later in the comparison with experiments. At temperatures above ~10,000 K the difference in the atom–molecule collision integrals does not influence the viscosity and heat conduction coefficients; here charged particle collisions start to play a noticeable role in transport processes.

The difference in the atom–atom collision integrals (see Figs. 3 and 4) does not influence the values of the viscosity and heat conduction coefficients at temperatures below 4500 K exactly as at temperatures above ~13,000 K, but results in a 8-10% discrepancy in λ_{eff} and up to 30% in μ in the intermediate domain of dissociation development and the initial stage of ionization. The influence of the spread in the atom–atom collision integrals on the heat conduction and viscosity coefficients of nitrogen is displayed in Figs. 6 and 7 and on the heat conduction of air in Fig. 8. Curve 1 is the computation by means of potentials obtained in the EGM approximation [28], while 2 is by potentials of [32] for identical collision integrals of the remaining components [29].

The collision integrals of charged particles whose interaction is associated with resonance charge transfer exceed the collision integrals of the components by several times for

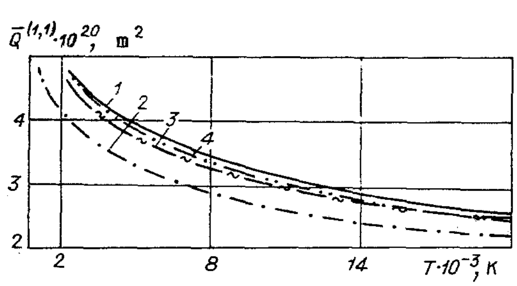

Fig. 4

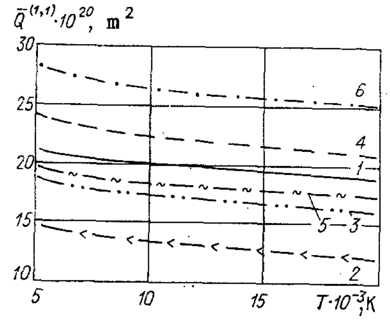

Fig. 5

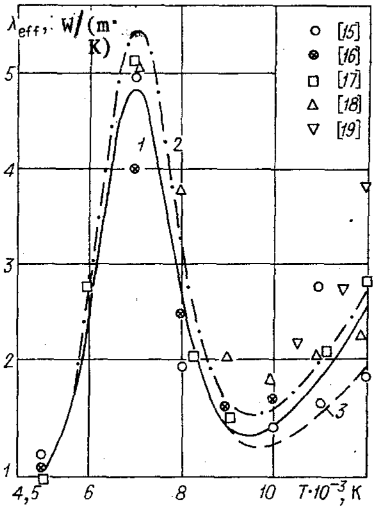

Fig. 6

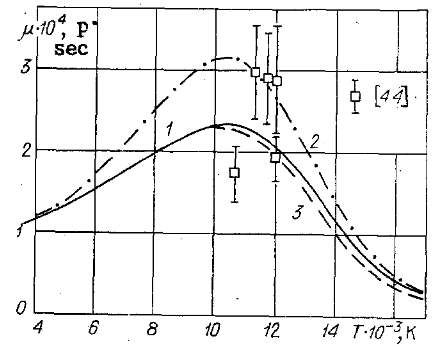

Fig. 7

TABLE 1

T, K	λ_{eff}, W/(m·K)			$\mu\cdot 10^4$, Pa·sec	
	[26]	[29]	Isolated AAP [29]	[26]	[29]
2000	9,135	0,138		0,687	6,94
3000	0,470	0,475		0,913	9,48
4000	0,564	0,593	0,543	1,180	1,23
5000	0,699	0,706	0,705	1,42	1,48
6000	2,36	2,36	2,36	1,67	1,72
7000	4,17	4,17	4,17	1,93	1,96
8000	2,28	2,28	2,28	2,11	2,11

ordinary elastic interaction; consequently, taking account of the resonance exchange processes is already necessary at ~9000-10,000 K temperatures for an insignificant percentile charged particle content in the mixture. The influence of the resonance exchange section on the accuracy of calculating the heat conduction and viscosity coefficients is shown in Figs. 6-9 for $p = 1.013\cdot 10^5$ Pa. Curve 1 in Fig. 6 is for a computation using the Capitelli [36] exchange section, while 3 is for a computation using the Smirnov [39] exchange sections. The difference in λ_{eff} associated with the utilization of different exchange sections is manifest in still a greater degree as the temperature rises. Presented in Figs. 8 and 9 are computations of the λ_{eff} for air and nitrogen, respectively, in the temperature domain to 20,000 K, where 1 is the computation over exchange sections [37] for $N-N^+$ pairs and Beebe [43] for $O-O^+$, 3 is over the exchange sections [39] and 5 is over the exchange sections [36]. The maximal spread in the air transport coefficients due to utilization of the exchange sections found by different investigation methods is up to 40-50% in the heat conduction coefficient and up to several percent in the viscosity coefficient. However, the discrepancy in λ_{eff} is not large when applying data with the best foundation on the exchange sections [37, 39] (within the limits of several percent).

TABLE 2

T, K	μ, μPa·sec					
	experiment	computation using data of				
	[42]	[26]	[29] %	[2] %	[32] %	[22] %
300	18,56	18,72	18,14(−2)	18,35(−1)	18,43(−0,7)	15,61(−15)
500	27,295	26,94	25,80(−5)	26,14(−4)	26,71(−1,8)	23,27(−14)
1000	43,08	42,97	42,10(−2)	41,27(−4)	44,19(−2,5)	39,99(−7)
1200	48,46	48,52	48,0(−0,9)	46,47(−4)	50,45(−4)	46,11(−5)
1400	53,64	53,81	53,7(0,1)	51,38(−4)	56,42(−4)	52,03(−5)
1500	56,18	56,35	56,5(0,4)	53,74(−4)	62,17(10)	54,92(−2)
2000	68,26	68,59	69,4(1,6)	64,97(−5)	73,11(7)	68,95(1)
2400	77,05	77,93	79,5(3)	73,62(−4)	83,51(8,4)	79,90(3,7)
2500	79,12	80,21	81,94(3,5)	75,80(−4)	86,06(8,8)	82,64(4)

TABLE 3

T, K	λ_{eff}, W/(m·K)				$\mu \cdot 10^4$, Pa·sec			
	[29]	[22]	isolated APP	Δ, %	[29]	[22]	isolated APP	Δ, %
3 000	0,470	0,543	0,451	+15÷−5	0,913	0,913	0,908	+2÷−1
4 000	0,564	0,632	0,565	+10÷+1	1,18	1,29	1,16	+9÷−1
5 000	0,699	0,749	0,633	+7÷−10	1,42	1,57	1,38	+10÷−3
6 000	2,36	2,50	2,02	+6÷−10	1,67	1,83	1,59	+9÷−5
7 000	4,17	4,44	3,48	+7÷−16	1,93	2,04	1,83	+5÷−5
8 000	2,28	2,42	1,93	+6÷−15	2,11	2,14	2,06	+1÷−1
9 000	1,21	1,24	1,12	+1÷−8	2,28	2,29	2,26	⩽1
10 000	1,37	1,38	1,35	⩽1	2,41	2,41	2,41	<1

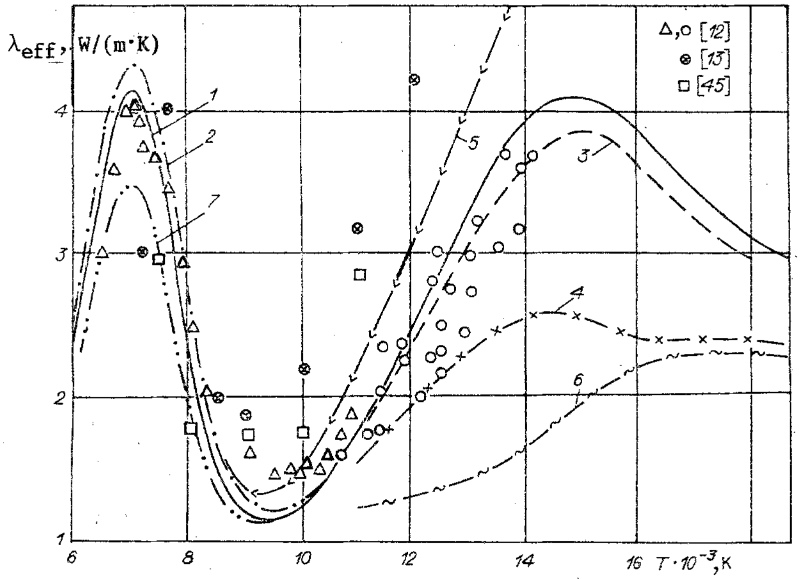

Fig. 8

Presented for comparison in Figs. 6-9 are results of experiments on the heat conduction coefficient of air [12, 13, 45], nitrogen [14-19], and viscosity of nitrogen [44]. Comparison of the viscosity and heat conduction coefficient computations for the existing spread in the particle collision integrals with experimental results could, in principle, be a confirmation of the correctness of selecting some initial data taken for the computation of the transport properties. Experimental data on the viscosity could be a good confirmation of the selection of the atom−atom collision integrals; however, the spread in the experimental points of μ (see Fig. 7) turns out to be of the same order as the spread in μ because of using different atom−atom collision integral data. It is seen from Fig. 8 that the best agreement with the maximal value of λ_{eff}^{max}(~4.02) obtained in experiments [12, 13] is observed in computations of the heat conduction coefficient if potentials of quantum mechanical computations [28] (curve 1) are used for the atom−atom interactions. From a comparison of the λ_{eff} for nitrogen with the experimental data (see Fig. 6), it is also seen that preference for the atom−atom interaction can be given to potentials of [28] as compared with [32]: the

TABLE 4

System	A, eV	$\alpha\cdot10^{10}$, m	System	A, eV	$\alpha\cdot10^{10}$, m
N—N	648,0	3,314	$O—O_2$	4652,0	4,051
O—O	1128,0	3,672	N—NO	393,3	2,954
N—O	855,0	3,493	O—NO	1887,0	3,671
$O—N^+$, $O^+—N$	1218,0	3,740	$N_2—N_2$	405,4	2,559
$O—O^+$ for $Q^{(2,s)}$	855,0	3,493	$O_2—O_2$	13310,0	3,918
$N—N^+$ for $Q^{(2,s)}$	923,4	3,562	$N_2—O_2$	2185,0	3,241
$N—N_2$	191,2	2,627	NO—NO	2295,0	3,261
$O—N_2$	890,0	3,345	$N_2—NO$	940,5	2,906
$N—O_2$	931,7	3,332	$O_2—NO$	55147,0	3,596

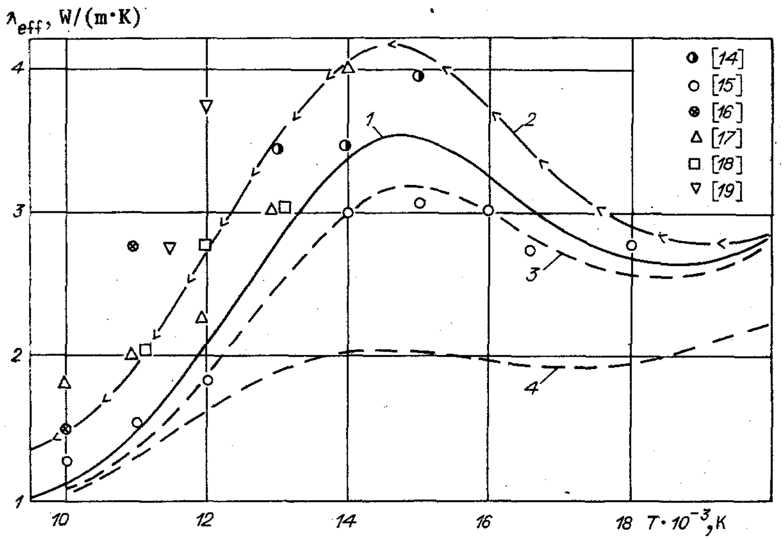

Fig. 9

majority of experimental points of λ_{eff} for nitrogen in the 6000-10,000 K temperature band lies below the curve computed with the potentials of [32]. The atom—molecule collision integrals used in these computations are taken from [29]. If atom—molecule collision integrals computed by means of potentials found from beam scattering experiments [22] are taken for calculation of λ_{eff}, then the value of the maximal coefficient λ_{eff}^{max} grows still more [up to 4.44 W/(m·K)] as compared with the experimental value (~4.02 W/(m·K)]. If the atom—atom potentials of [32] are applied simultaneously with the atom—molecule interaction potentials obtained from beam scattering, then λ_{eff}^{max} will be still higher. If interaction potentials found in the AAP model with isolated atom potentials (curve 2 in Fig. 2) are taken for the atom—molecule collision integrals, then the value of λ_{eff}^{max} will drop to 3.48 W/(m·K) and the corresponding curve of λ_{eff} (7 in Fig. 8) will pass below the experimental points.

Experimental data on the heat conduction coefficient in the temperature domain above 11,000 K can be the selection criterion for the resonance exchange section in the computation of collision integrals between ions and similar atoms. The spread in the experimental points on the heat conduction coefficient generally exceeds the discrepancy in the results of numerical computations of λ_{eff} because of the spread in the ion-similar atom collision integrals when using different methods of computing the exchange sections, so that it is difficult to make unique deductions on the recommendations of some exchange sections. Even if points exceeding the results of [12, 14] because of the possible exaggeration of the experimental values of the heat conduction coefficient whose thorough analysis is carried out in [14] are eliminated for the analysis from a series of experimental points on the heat conduction coefficient of nitrogen (see Fig. 9) at temperatures T ~ 12,000-14,000 K and of air (see Fig. 8) at T ~ 11,000-12,000 K, then the best agreement with experiments is given by a computation in which exchange sections found by the most sequential quantum mechanical computations [37] (curve 1 in Figs. 8 and 9) are used.

Therefore, the viscosity and heat conduction transport coefficients represented in Figs. 6-9 turn out to be in the best agreement with data of experiments both in comparison with

TABLE 5

Object	Δ, %			
	T, K			
	300—2500	3000—7000	8000—11000	12000—18000
$Q^{l,s}$ (molecule—molecule)	1,5	2—5	10	10
$Q^{l,s}$ (atom—molecule)	—	5	5	5
$Q^{l,s}$ (atom—atom)	—	2	3	3
$Q^{l,s}$ (atom—ion)	—	12	12	15
λ_{eff}	1,5	2—5	8	13
μ	1,5	2	10	10

computations performed with another set of collision integrals and in comparison with computations [46] (curve 4 in Figs. 8 and 9) which are evidently lowered since the computations of [46] are executed in a first nonzero approximation and of [47] (curve 6 in Fig. 8). This agreement can be an indirect confirmation of the possibility of applying models taken in the computation of air component collision integrals for the broader circle of multicomponent mixtures:

1) When computing the transport properties of chemically equilibrium mixtures, the interaction of neutral components—molecules can be given by a potential in which the domain of long-range interactions should be sufficiently strictly based, while more approximate methods are admissible for the description of short-range forces;

2) The appearance of long-range forces in the computation of effective transport coefficients of chemically equilibrium mixtures is not essential in the interaction of neutral atoms and their ions; consequently, selection of the model to describe long-range forces is of no value in principle;

3) Quantum mechanical methods for the computations of scattering sections of atoms and their ions are more preferable as compared with semiempirical methods which, it is true, yield fair agreement with experiment in a number of cases; but only by sequential quantum mechanical computations can the errors admitted in calculating the properties be estimated;

4) Resonance exchange processes of the neutral with similar charged particles exert substantial influence in the computation of properties of partially ionized mixtures since the sections Q_{ex} exceed by several times Q^{ℓ}_{ela} computed without taking exchange into account and the accuracy of computing the transport properties in this domain is determined mainly by the accuracy of the resonance exchange sections.

The collision integrals of the neutral components taken for the computation of the air transport properties are approximated by simple algebraic functions with ~1% error for temperatures above 2000 K:

$$Q^{(1,1)} = 0.5816\pi\zeta^{2.2405} \exp(-0.01337\zeta)/\alpha^2,\ Q^{(2,2)} = \omega^{(2,2)} Q^{(1,1)},$$
$$\omega^{(2,2)} = 1.539 - 0.0672\zeta + 0.0032\zeta^2,\ \zeta \leqslant 8.0,$$
$$\omega^{(2,2)} = 1.331 - 0.0166 \ln\zeta,\quad \zeta > 8.0.$$

Here $\zeta = \ln(A/kT) = \ln[1.1604A/(T/10^4)]$; A and α are parameters (their values are given in Table 4).

Approximations of $\omega^{(l,s)} = Q^{(l,s)}/Q^{(1,1)}$ of the next orders in ℓ and s are presented in [26]. The collision integrals for the resonance charge exchange are approximated by the relations:

For $N-N^+$ (over exchange sections [37])

$$\overline{Q}^{(1,1)} = 20.0 - 2.5 \lg(T/10^4) - 8.07 \lg^2(T/10^4)(10^{-20}\text{m}^2),$$
$$\overline{Q}^{(1,2)} = 0.977\overline{Q}^{(1,1)},\ \overline{Q}^{(1,3)} = 0.960\overline{Q}^{(1,1)},\ \overline{Q}^{(1,4)} = 0.958\overline{Q}^{(1,1)},$$
$$\overline{Q}^{(1,5)} = 0.955\overline{Q}^{(1)},\ \overline{Q}^{(3,3)} = \overline{Q}^{(1,1)};$$

for $O-O^+$ (over exchange sections [43])

$$\bar{Q}^{(1,1)} = 13.4 - 4.28\,\lg(T/10^4) + 3.403\,\lg^2(T/10^4)(10^{-20}\ \mathrm{m}^2),$$
$$\bar{Q}^{(1,2)} = 0.97\bar{Q}^{(1,1)},\ \bar{Q}^{(1,3)} = 0.95\bar{Q}^{(1,1)},\ \bar{Q}^{(1,4)} = 0.94\bar{Q}^{(1,1)},$$
$$\bar{Q}^{(1,5)} = 0.93\bar{Q}^{(1,1)},\ \bar{Q}^{(3,3)} = \bar{Q}^{(1,1)}.$$

Thus, despite the existence of a significant spread in the initial information on particle interaction (the indeterminacy in the potential energy is up to 50% and more in certain ranges of $\{R\}$), a number of calculational procedures reduce the total error in the computation of the properties: for the triple integration of $Q^{(\ell,s)}(T)$ in calculating the angles $\chi(b, g)$, the potential $V(R)$ given outside the domain of greatest proximity $\{R_m\}$ influences slightly, and different kinds of models turn out to be suitable for extrapolation of the potential energy; the contribution of small angles to the integral is not essential for computation of the sections $Q^{\ell}(E)$; the contribution of sections for large and small energies is not essential in integration of the energy sections. Moreover, the indeterminacy in the collision integrals for the computation of transport properties of multicomponent mixtures of chemically reacting gases is leveled by the presence of molecules, atoms, ions, and electrons in individual temperature bands for individual components. Comparison of the collision integrals computed by known methods with the best foundations to obtain the interaction potentials and comparison of the results of computing the transport coefficients in which different sets of collision integrals are used with data of experiments on the heat conduction and viscosity of air and nitrogen within broad temperature ranges showed the limits of the possible errors in the transport coefficients admitted in the computations because of inaccurate initial information. The estimates obtained for the probably allowable errors in the collision integrals $Q^{(\ell,s)}(T)$, taken for the computation of the transport properties, and in the coefficients λ_{eff} and μ for air are presented in Table 5.

LITERATURE CITED

1. J. Ferziger and J. Capper, Mathematical Theory of Transport in Gases [Russian translation], Mir, Moscow (1976).
2. J. Hirschfelder, C. Curtiss, and R. Bird, Molecular Theory of Gases and Fluids [Russian translation], IL, Moscow (1961).
3. R. S. Devoto, "Transport properties of ionized monatomic gases," Phys. Fluids, 9, No. 16 (1966).
4. I. A. Sokolova, "Transport coefficients and collision integrals of air and its components," Physical Kinetics [in Russian], No. 4, Inst. Teor. Prikl. Mekh., Sib. Otd. Akad. Nauk SSSR, Novosibirsk (1974).
5. A. F. Kolesnikov and G. A. Tirskii, "Hydrodynamics equations for partially ionized multicomponent gas mixtures with transport coefficients in high approximations," Molecular Gasdynamics. Fifth All-Union Conf. on Rarefied Gas Dynamics and Molecular Gas Dynamics [in Russian], Nauka, Moscow (1982).
6. S. A. Vasil'evskii, I. A. Sokolova, and G. A. Tirskii, "Exact equations and transport coefficients for a multicomponent gas mixture and partially ionized plasma," Zh. Prikl. Mekh. Tekh. Fiz., No. 4 (1984).
7. M. Mitchner and C. Kreuger, Partially Ionized Gases [Russian translation], Mir, Moscow (1976).
8. L. Spitzer and R. Harm, "Transport Phenomena in a completely ionized gas," Phys. Rev., 89, No. 5 (1953).
9. E. A. Mason and L. Monchick, "Heat conductivity of polyatomic and polar gases," J. Chem. Phys., 36, No. 6 (1962).
10. S. A. Vasil'evskii, I. A. Sokolova, and G. A. Tirskii, "Determination and calculation of the effective transport coefficients for chemically equilibrium flows of partially dissociated and ionized gas mixtures," Zh. Prikl. Mekh. Tekh. Fiz., No. 1 (1986).
11. É. I. Asinovskii and E. P. Pakhomov, "Analysis of experimental data on gas viscosity in the high-temperature domain," Teplofiz. Vys. Temp., 8, No. 4 (1970).
12. É. I. Asinovskii and V. I. Shabashov, "Experimental investigation of the electrical conductivity and heat conductivity coefficients of an air plasma," Teplofiz. Vys. Temp., 7, No. 2 (1969).
13. R. S. Devoto, U. H. Bauder, et al., "Air transport coefficients from electric arc measurements," Phys. Fluids, 27, No. 4 (1978).

14. É. I. Asinovskii, E. V. Drokhanova, et al., "Experimental and theoretical investigation of heat conductivity and total radiation coefficients of a nitrogen plasma," Teplofiz. Vys. Temp., 5, No. 5 (1967).
15. W. Hermann and E. T. Schade, "Transportfunktionen von Stickstoff bis 26,000 K," Z. Phys., 233, 333 (1970).
16. J. Von Uhlenbusch, "Berechnung der Hateralfunktionen eines Stickstoff und Argon Plasmas aus gemessenen Bogendata," Z. Phys., 179, 347 (1964).
17. J. C. Morris, R. R. Rudis, and J. M. Yos, "Measurements of electrical and thermal conductivity of hydrogen, nitrogen, and argon of high temperatures," Phys. Fluids, 13, No. 3 (1970).
18. U. Plantikow, "Bestimmung von Transportkoeffizienten des Stickstoffs bis 13,000 K," Z. Phys., 237, 388 (1970).
19. P. M. Schreiber, A. M. Hunter, and K. R. Benedetto, "Measurement of nitrogen plasma transport properties," AIAA J., 10, No. 5 (1972).
20. J. C. Raich and N. S. Gillis, "The anisotropic interaction between nitrogen molecules from solid state data," J. Chem. Phys., 66, 846 (1977).
21. B. Brunetti and G. Liuti, "Study of the interactions of atomic and molecular oxygen with O_2 and N_2 by scattering data," J. Chem. Phys., 74, No. 12 (1981).
22. V. B. Leonas, "Investigation of short-range intermolecular forces," Usp. Fiz. Nauk, 107, No. 1 (1972).
23. R. H. Ree and N. W. Winter, "Ab initio and Gordon–Kim interaction potentials for two nitrogen molecules," J. Chem. Phys., 73, No. 1 (1980).
24. T. R. McRury, W. A. Steel, and B. J. Berne, "Intermolecular potential models for anisotropic molecules with applications to N_2, CO_2, and benzene," J. Chem. Phys., 64, No. 4 (1976).
25. R. M. Berns and A. van der Avoird, "N_2–N_2 interaction potential from ab initio calculation to the structure of $(N_2)_2$," J. Chem. Phys., 72, No. 11 (1980).
26. O. A. Gordeev, A. P. Kalinin, A. L. Komov, et al., "Interaction potentials, elastic sections, collision integrals of air components for temperatures to 20,000 K. Surveys on the thermophysical properties of substances" [in Russian], TFTs, No. 5, Inst. Vys. Temp. Akad. Nauk SSSR, Moscow (1986).
27. J. C. Rainwater, L. Biolsi, and K. J. Biolsi, "Transport properties of ground state nitrogen atoms," J. Chem. Phys., 79, 1462 (1983).
28. V. I. Gaidaenko and V. K. Nikulin," Born–Mayer interatomic potential for atoms with z = 2 to z = 36," Chem. Phys. Lett., 7, 360 (1970).
29. I. A. Sokolova and G. A. Tirskii, "Computation and approximation of collision integrals of mixture components containing O, H, C, N, F, Na, S, Si atoms and their compounds," Report No. 2857 [in Russian], Moscow Univ. Inst. of Mechanics (1983).
30. T. Holstein, "Mobilities of positive ions in their parent gases," J. Phys. Chem., 56, No. 7 (1952).
31. Yu. N. Belyaev, E. G. Shapiro, and K. V. Romashin, "Collision integrals for neutral dissociating air components," Report No. 2043 [in Russian], Moscow Univ. Inst. of Mechanics (1978).
32. S. J. Cubley and E. A. Mason, "Atom–molecular and molecular–molecular potentials and transport collision integrals for high-temperature air species," Phys. Fluids, 18, 1109 (1975).
33. J. T. Vanderslice, E. A. Mason, and E. R. Lippincott, "Interactions between ground-state nitrogen atoms and molecules: the N–N, N–N_2, N_2–N_2 interactions," J. Chem. Phys., 30, 129 (1959).
34. J. T. Vanderslice, E. A. Mason, and W. G. Marsch, "Interactions between oxygen atoms and molecules: O–O, O–O_2," J. Chem. Phys., 32, No. 2 (1960).
35. M. Capitelli and V. E. Ficocelli, "Collisions integrals of oxygen atoms in different electronic states," J. Phys. B., 5, 2066 (1972).
36. M. Capitelli and R. S. Devoto, "Transport coefficients of high-temperature nitrogen," Phys. Fluids, 16, 1835 (1973).
37. M. Capitelli and U. Lamanna, "The gerate-ungerate splitting N_2^+ potentials: effect on the resonant charge transfer cross sections on nitrogen atoms," Chem. Phys., 19, 269 (1977).
38. E. W. Thulstrup and A. Andersen, "Configuration interaction studies of bound low-lying states of N_2^-, N_2^+, N_2^{2+}, and N_2," J. Phys. B., 8, 965 (1975).
39. E. A. Duman and B. M. Smirnov, "Tables of resonance charge transfer sections of ions by atoms," Teplofiz. Vys. Temp., 12, No. 3 (1974).

40. H. Knoff, E. A. Mason, and J. T. Vanderslice, "Interaction energies, charge-exchange cross sections, and diffusion cross sections for $N-N^+$ and $O-O^+$ collisions," J. Chem. Phys., 40, 3548 (1964).
41. V. A. Belyaev, B. G. Brezhnev, and E. M. Erastov, "Resonance charge transfer of carbon and nitrogen ions at low energies," Zh. Éksp. Teor. Fiz., 54, No. 5 (1968).
42. V. E. Lyusternik and A. V. Lavushchev, "Survey and experimental refinement of data on air and argon viscosities for temperatures to 2000 K and atmospheric pressure," Thermodynamic Properties of Substances and Materials [in Russian], No. 12, Standartov, Moscow (1978).
43. N. H. F. Beebe, E. W. Thulstrup, and A. Andersen, "Configuration interactions of low-lying electronic states of O_2, O_2^+, O_2^{2+}," J. Chem. Phys., 64, 2080 (1976).
44. P. M. Schreiber, A. M. Hunter, and K. R. Benedetto, "Argon and nitrogen plasma viscosity measurements," Phys. Fluids, 12, 2696 (1971).
45. G. Mekker and U. Bauder, "Determination of transport properties of a plasma," Properties of a Low-Temperature Plasma and Methods of Diagnosing It [in Russian], Nauka, Novosibirsk (1977).
46. J. M. Yos, "Revised transport properties for high-temperature air and its components," RT-65, AVCO Corp., Wilmington, Mass (USA) (1965).
47. P. P. Kulik and Y. G. Panevin, "Transport properties of thermally ionized air," 8th Intern., Conf. on Phenomena in Ionized Gases, Vienna (1967).

DYNAMICS OF A MICROWAVE DISCHARGE IN A HIGH-PRESSURE MOLECULAR GAS

E. Ya. Kogan and B. Yu. Kuzin

UDC 537.2+533.591

1. A high-frequency discharge in a dense gas ($\nu_e > \omega$) and subthreshold field is formed in two stages. Initially, a non-self-consistent discharge initiated by an external ionization source is excited. The ionization-superheating instability being developed in it transfers it into the self-consistent mode. The same stages govern transport breakdown in the gas, i.e., the formation of ionization waves. A non-self-consistent discharge in unperturbed gas domains is associated here with energy transport from the steady-state discharge domain [1-3]. The self-consistent discharge goes over into the mode in the nonlinear stage of ionization-superheating instability, in its saturation stage. Consequently, analysis of this stage permits estimation of the steady-state discharge parameters and its space–time configuration.

The nonlinear stage of the ionization-superheating instability is characterized by the fact that the exponential growth of the plasma density is replaced by explosive, and under these conditions particle and heat diffusion does not stabilize the instability [4]. Here the evolution of the perturbation in the nonlinear mode is kept in mind with the exacerbation [5-7] in which instability development in the dissipative system results in diminution of the space and time scales of the parameter distribution.

In this stage, the equation [4]

$$\partial P/\partial t = \partial^2 P/\partial x^2 + f(P) \tag{1.1}$$

follows under sufficiently general assumptions on gas and plasma parameter evolution [f(P) is a nonlinear function of the parameter P). It can be shown that under gas breakdown conditions in a subthreshold microwave field under sufficiently general assumptions $f(P) = P^\alpha$ ($\alpha > 1$). Then a simple analysis of the dimensionality of the equation permits estimation of the space Δx and time Δt scales of the distribution $\Delta t \sim P^{-(\alpha-1)}$, $\Delta x \sim P^{-(\alpha-1)/2}$, from which there results that the instability is not saturated in the nonlinear mode while the perturbation collapses.

The analysis presented does not take into account that electromagnetic field interaction with a plasma is characterized by proper spatial scales, the skin layer λ and the field energy absorption length $1/\mu$. Since $\lambda \lesssim 1/\mu$, the skin-layer corresponds to the dimension of the effective field interaction with the plasma. Such a scale asymptotically governs the system behavior by subordinating itself to space–time scales of nonlinear diffusion processes.

Kuibyshev. Translated from Zhurnal Prikladnoi Mekhaniki i Tekhnicheskoi Fiziki, No. 3, pp. 28-34, May-June, 1988. Original article submitted March 3, 1987.

0021-8944/88/2903-0338$12.50